Coexpression of Insulin Receptor-Related Receptor and Insulin-Like Growth Factor 1 Receptor Correlates with Enhanced Apoptosis and Dedifferentiation in Human Neuroblastomas

Axel Weber,[1] Christine Huesken,[1] Eckhard Bergmann,[1] Wieland Kiess,[2] Nina M. Christiansen,[1] and Holger Christiansen[1]

[1]University Children's Hospital, Marburg, and [2]Children's Hospital, Leipzig, Germany

ABSTRACT

Purpose: **We compared the expression of the insulin receptor-related receptor (IRR) in primary human neuroblastomas with other biological and clinical parameters and the impact of its expression on prognostic outcome.**

Experimental Design: **We studied 49 neuroblastomas of different clinical stages and histological subtypes for (*a*) IRR, insulin-like growth factor 1 receptor (IGF-1R), TrkA, p75 neurotrophin receptor, and MYCN mRNA expression by reverse transcription-PCR; (*b*) *MYCN* gene amplification by Southern blot analyses; (*c*) cyclin A protein expression by Western blot analyses indicating proliferation rate; and (*d*) apoptotic index (AI) by terminal deoxynucleotidyl transferase (Tdt)-mediated dUTP nick end-labeling assay.**

Results: **IRR mRNA expression was found in 25 (51%) neuroblastomas and correlated with stages 1, 2, 3, and 4S disease and with age ≤12 months at diagnosis. IRR was expressed predominantly in neuroblastomas without *MYCN* gene amplification and coexpressed with IGF-1R, TrkA, and p75 neurotrophin receptor. IRR mRNA expression also correlated with an undifferentiated histology but not with the proliferation rate. In coexpression with IGF-1R, the IRR was associated with enhanced AI. IRR expression was significantly correlated with a good prognosis in all 49 neuroblastomas (6-year survival probability, 91.8% *versus* 49.7% for IRR nonexpression; $P = 0.003$).**

Conclusion: **IRR expression is a new marker for a favorable prognosis in neuroblastoma that is independent of *MYCN* amplification and age at diagnosis. Our data suggest an influence of IRR on IGF signaling via IGF-1R because coexpression of these two receptor tyrosine kinases was significantly correlated with an undifferentiated histology, a high AI, and an advanced survival probability.**

INTRODUCTION

Neuroblastoma is the third most common pediatric cancer and is responsible for ~15% of all childhood cancer deaths. It is an embryonal tumor of the postganglionic sympathetic nervous system, which most commonly arises in para- and prevertebral ganglia and in the adrenal gland. The 6-year survival probability of all patients with neuroblastoma is ~60% (own data based on 2030 patients registered from 1980 to 2003). In addition to clinical markers such as stage and age at diagnosis, biological tumor markers have gained increasing importance in determining the prognostic outcome for patients with neuroblastoma. The most extensively studied biological marker for an unfavorable prognostic outcome in patients with neuroblastoma is the amplification of the *MYCN*[3] oncogene (1–3).

MYCN is differentially expressed in neuroblastomas with or without *MYCN* gene amplification and in different clinical stages (4). However, the prognostic impact of MYCN expression is controversial and has not been shown to be of prognostic relevance in most studies (5, 6). Among other biological markers for a favorable prognostic outcome in neuroblastoma are expression of the high-affinity nerve growth factor receptor TrkA (7) and the low-affinity nerve growth factor receptor p75NTR (8–10).

The IGF-1R is of prognostic relevance in a variety of tumor entities and influences apoptosis, differentiation, and proliferation in coexpression with other RTKs (11, 12). In neuroblastoma cells, expression of IGF-1R has been implicated in growth-promoting and antiapoptotic signaling (13). In contrast to its implication in cell survival, proapoptotic action by IGF-1R has been seen in cells that have been triggered to undergo apoptosis through receptors of the death receptor family, such as TNF receptors or p75NTR (14).

Recently, the IRR has been identified as an additional member of the insulin RTK family (15, 16). However, its ligand and biological functions are still unknown. Various ligands activating the IR or the IGF-1R, such as proinsulin, insulin,

Received 3/18/03; revised 7/22/03; accepted 8/4/03.

Grant support: This work was supported by the "Deutsche Krebshilfe" (10-1116-Ki2) W. K.'s laboratory is supported by IZKF, Leipzig, Germany. This work contains parts of the doctoral theses of A. W. and C. H. The costs of publication of this article were defrayed in part by the payment of page charges. This article must therefore be hereby marked *advertisement* in accordance with 18 U.S.C. Section 1734 solely to indicate this fact.

Requests for reprints: Holger Christiansen, M.D., Ph.D., Universitaetskinderklinik, Deutschhausstrasse 12, D-35037 Marburg, Germany. Phone: 49-6421-28-62671; Fax: 49-6421-28-66824; E-mail: Holger.Christiansen@mailer.uni-marburg.de; Internet: http://www.neuroblastom.info/.

[3] The abbreviations used are: MYCN, avian myelocytomatosis viral-related oncogene-neuroblastoma derived; TrkA, tyrosine receptor kinase A; P75NTR, P75 neurotrophin receptor; IGF-1R, insulin-like growth factor-1 receptor; RTK, receptor tyrosine kinase; TNF, tumor necrosis factor; IRR, insulin receptor-related receptor; DSR, diffuse-stroma-rich; SP-D, stroma-poor-differentiated; SP-U, stroma poor-undifferentiated; TUNEL, terminal deoxynucleotidyl transferase (Tdt)-mediated dUTP nick end-labeling; M/A, ratio of MYCN to β-actin; AI, apoptotic index; GAPDH, glyceraldehyde-3-phosphate dehydrogenase.

IGF-1, IGF-2, and relaxin, are not able to bind the extracellular domain and activate IRR (17, 18). The functional potential of the tyrosine kinase domain of the IRR was demonstrated by use of receptor hybrids of a known extracellular domain and the intracellular domain of the IRR. Thus, IR substrate-1 and -2 have been identified as receptor substrates of the IRR, implicating a role for the IRR in influencing downstream signaling pathways such the phosphatidylinositol 3′-kinase and the mitogen-activate protein kinase pathway (17).

In contrast to the widespread patterns of expression of the homologous IR and IGF-1R, IRR demonstrates a very restricted cellular distribution in a subset of tissues of neuronal origin, where its appearance is closely associated to that of IR, IGF-1R, and the nerve growth factor receptor TrkA (19, 20). IRR and TrkA appear early in the embryonal development of dorsal root and trigeminal neurons and later, near the time of birth, in sympathetic neurons. This association is highly selective: TrkA mRNA is not detected anywhere else in the developing nervous system in the absence of coordinate IRR expression (20, 21). Furthermore, it was shown recently that IRR is also coexpressed with IGF-1R in neuroblastoma cell lines (22). Coexpression of receptors of the IR family has been shown to influence activation of downstream signaling pathways and cellular biological functions, which might be explained by heterodimerization of the expressed receptor monomers on the cell surface, resulting in different ligand-binding affinities and autophosphorylation status (23–26).

These observations prompted us to study the possible role of IRR expression in primary neuroblastomas. We examined the relationship of IGF-1R, TrkA, and p75NTR mRNA expression with the expression of IRR and correlated this expression pattern to biological effects such as proliferation, apoptosis, and morphological differentiation. We also asked whether *MYCN* amplification/expression status correlates with the IRR expression pattern and whether the IRR might have any prognostic impact on patients with neuroblastoma.

MATERIALS AND METHODS

Patients. We studied tumor specimens from 49 children with neuroblastoma who had been diagnosed in Germany from 1989 to 1997. All neuroblastoma diagnoses were confirmed by histological assessment of a tumor specimen obtained at surgery. The tumors were classified according to the INSS criteria (27). We studied 8 stage 1 (16%), 7 stage 2 (14%), 9 stage 3 (18%), 14 stage 4 (28%), and 11 stage 4S (22%) tumors. The relative incidence rate in our study reflects the relative incidence rate of neuroblastomas in Germany within the investigated time period (1990–1997): stage 1 (19%), stage 2 (12%), stage 3 (20%), stage 4 (39%), and stage 4S (10%).

The median age of the patients at diagnosis was 12.9 months (range, 0.2–131.6 months). Thirteen (26.5%) tumors had a DSR histology, six (12.2%) were SP-D, and 30 (61.2%) were SP-U (28). All patients were treated in a stage-specific manner according to previously described protocols (29). The survival probability of our study population calculated with Kaplan–Meier analysis was 70.5%.

Tissue Preparation. The neuroblastoma specimens were frozen in liquid nitrogen and stored at −80°C for PCR and Southern and Western blot analyses. Portions of the samples (50–60 mg) were fixed in 10% buffered formalin. Serial sections 4-μm in thickness were cut from the same blocks, mounted on poly-L-lysine-coated slides, and used for H&E staining and *in situ* end-labeling of DNA (TUNEL assay).

RNA Extraction and Reverse Transcription. Tumor samples (100 mg each) were homogenized in 1000 μl of RNA-zol-B (Biotecx Laboratories Inc., Houston, TX). RNA was isolated after the addition of chloroform according to the guanidinium-isothiocyanate method (30) and finally precipitated with isopropanol. After centrifugation (14000 × *g* for 20 min), the pellet was washed twice with 70% ethanol, vacuum-dried, and dissolved in 50–80 μl of RNase-free distilled water.

We incubated 7500 ng of total RNA at 70°C for 10 min with 1.5 μl of RNase inhibitor (40 units/μl; Promega), 2.5 μl of oligo-primer-p(dT)15 (0.1 nmol/μl; Boehringer-Mannheim) and distilled water in a volume of 42 μl; we then cooled the mixture to 4°C. First-strand cDNA was synthesized with 1.5 μl of Moloney murine leukemia virus reverse transcriptase (Super-Script-II; Invitrogen) in a total volume of 75 μl [15 μl of 5× first-strand buffer (Invitrogen), 7.5 μl of dithiothreitol (0.1 M; Invitrogen), 3 μl of BSA, 1.5 μl of each deoxynucleotide triphosphate (0.01 μmol/μl; Perkin-Elmer), and 0.5 μl of RNasin]. Reverse transcription was performed for 10 min at 25°C and 60 min at 42°C, and finally for 15 min at 75°C to inactivate the enzyme.

Primer Search. Specific primers for the amplification of IRR, IGF-1R, p75NTR, TrkA, MYCN, and β-actin were searched with OLIGO 6.0 (Medprobe); the specificity was controlled with BLAST 2.0 (http://www.ncbi.nlm.nih.gov/blast/blast.cgi). To avoid coamplification of contaminating DNA, primers were located in two subsequent exons. All PCR products were sequenced by the dye-termination procedure on a ALF-express with 5′-Cy5-labeled primers according to the manufacturer's protocol (Pharmacia Biotech); the results were compared with the respective published sequence data (http://www.ncbi.nlm.nih.gov/GenBank/index.html; Table 1).

PCR. PCR was performed in a total volume of 50 μl containing 5 μl of 10× PCR buffer, 2.5 units of *Taq*-polymerase-k (MoBiTec), 1 μl of each deoxynucleotide triphosphate (Perkin-Elmer), 50 pmol of each primer, 200 ng of total cDNA, 1 μl of formamide (Sigma), and 33 μl of distilled water.

The primer sequences and individual PCR conditions (annealing and elongation temperature, time, and cycle number) for each PCR are listed in Table 1. In every PCR, an initial denaturation step at 95°C for 3 min was performed, denaturation during cycling was performed at 95°C for 30 s, and the last cycle was followed by an elongation step at 72°C for 7 min. The reaction was then cooled to 4°C.

In the semiquantitative PCR of *MYCN* relative to β-*actin* (M/A), the first 5 cycles were done only with the *MYCN* primers. After the reaction was cooled to 4°C and the β-actin primers were added, the reaction was continued for 28 cycles, as described by Kinoshita *et al.* (31). PCR conditions have been established for both gene fragments to be in the logarithmic phase at the time of analysis. After agarose gel electrophoresis, the level of *MYCN* expression in each tumor was determined by densitometry and was expressed as the M/A ratio. *MYCN* ex-

Table 1 PCR product length, primer sequences, and PCR conditions

Gene		Primer sequences	PCR conditions
β-*actin*	Upper	5′-ATCTGGCACCACACCTTCTACAATGAGCTGCG-3′	64.5°C for 75 s; 72°C for 90 s; 28 cycles
(838 bp)	Lower	5′-CGTCATACTCCTGCTTGCTGATCCACATCTGC-3′	
MYCN	Upper	5′-AGCGGCGGCGACCACAAGGC-3′	64.5°C for 75 s; 72°C for 90 s; 5 + 28 cycles
(399 bp)	Lower	5′-CGAGTCAGAGTTTCGGGGGCTCAAGC-3′	
p75NTR	Upper	5′-CTGCAACCTGGGCGAGGGTGT-3′	63°C for 60 s; 72°C for 90 s; 40 cycles
(470 bp)	Lower	5′-CTGGGGGTGTGGACCGTGTAA-3′	
TrkA	Upper	5′-GCGCAGAGAACCTGACTGAGCT-3′	60°C for 60 s; 72°C for 90 s; 40 cycles
(442 bp)	Lower	5′-ACGTCGTCCCCCACATCCA-3′	
IRR	Upper	5′-AGGACGGCGACCTCTACCTCAAT-3′	62°C for 60 s; 72°C for 90 s; 40 cycles
(597 bp)	Lower	5′-TGAGTCCGTTGGGGTCTGGTG-3′	
IGF-IR	Upper	5′-ACTTCTGCGCCAACATCCTCA-3′	60°C for 60 s; 72°C for 90 s; 40 cycles
(572 bp)	Lower	5′-CCCTTTAGTCCCCGTCACTTCC-3′	

pression was defined as high for M/A at or above the median and as low for M/A below the median expression level.

Relative to common housekeeping genes (β-*actin* and *GAPDH*), the investigated receptors were found to be expressed at lower levels. Thus, semiquantification of receptor RNA expression was difficult and inaccurate, particularly in comparison with the *MYCN*/β-*actin* PCR. We decided to use a common cDNA-specific PCR with higher cycle number (up to 40) to avoid false-negative results. For a loading control, we equalized the amount of cDNA from each tumor with a *GAPDH* PCR for 26 cycles, which gave comparable specific bands (data not shown). The β-*actin* band in the *MYCN*/β-*actin* PCR was then used as an additional control. Each specific band was regarded as positive expression. Each tumor that was PCR negative was controlled in a second PCR for 50 cycles. None of the controlled tumors turned positive (Fig. 1).

Gel Electrophoresis. The amplified PCR fragments (10 μl of the PCR products) were separated on a 2% agarose gel by electrophoresis, identified by ethidium bromide staining, and documented by the Image Master VDS software (Pharmacia).

***MYCN* Amplification.** For the detection of *MYCN* amplification, the pNB-1 probe (*MYCN* is localized on 2p24.1; ATCC 41011) was used; control hybridization for a single-copy signal was performed with HuCK (IGKC is the immunoglobulin κ constant region, localized on 2p12; ATCC 59172).

DNA Isolation and Southern Blot Analysis. High-molecular-weight DNA was isolated by proteinase K digestion and phenol–chloroform extraction according to standard procedures. We digested 10 μg of DNA from each sample with *Eco*RI, and fragments were separated by 0.8% agarose gel electrophoresis. The DNA was then transferred to Gene Screen Plus membranes (DuPont) by vacuum-blotting (Pharmacia) according to the specifications of the manufacturer. Prehybridization and hybridization were performed according to standard procedures. Filters were washed twice in 0.1× SSC and 0.1% SDS at room temperature for 20 min and three times at 65°C for 30 min. After a brief rinse in 0.1× SSC, autoradiography was performed at −70°C with Kodak XAR-5 film (Fig. 1).

Western Blot Analysis. Cellular protein was extracted by lysing 30 mg of tumor tissue with 300 μl of lysis buffer [NP-40 + 4: 150 mM NaCl, 1% (v/v) NP-40, 50 mM Tris-buffer (pH 8), 5 mg/ml aprotinin, 5 mg/ml leupeptin, 1 mg/ml pepstatin, 0.2 M phenylmethylsulfonyl fluoride]. We separated 30 μg of protein in a 12% gradient SDS–polyacrylamide gel and electroblotted the bands to Hybond-Enhanced Chemiluminescence (ECL) nitrocellulose membrane (Amersham Corp., Arlington Heights, IL). After the membranes were blocked with

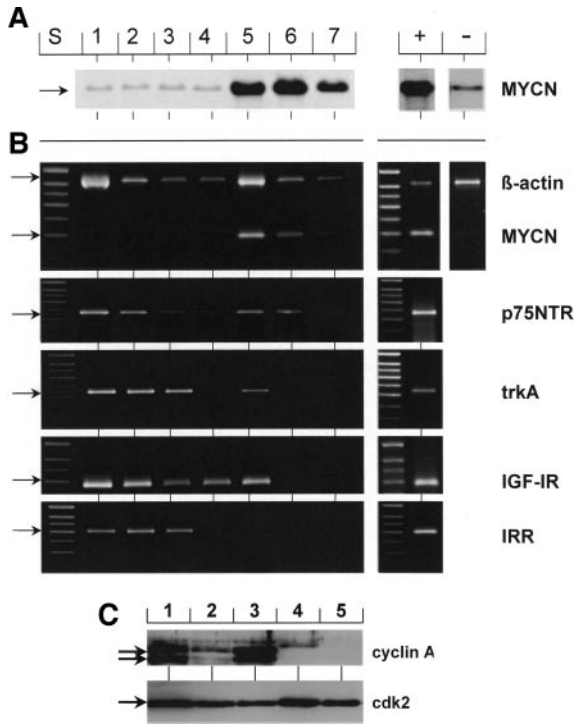

Fig. 1 *A*, seven representative neuroblastomas, examined for MYCN amplification by Southern blot analyses. *Lanes 1–4*, *MYCN* single-copy tumors; *Lanes 5–7*, *MYCN*-amplified tumors. Amplification-positive control (*Lane +*), IMR32 *MYCN*-amplified cell line; negative control (*Lane −*), SHEP *MYCN* single-copy cell line. *B*, same neuroblastomas as in *A*, examined by reverse transcription-PCR for receptor and *MYCN* mRNA expression. Expression of *GAPDH* (data not shown) and β-*actin* was used as an internal control. *Lane S*, length standard. For *MYCN* expression, IMR32 and SHEP cell line cDNAs were used as the positive and negative controls, respectively; for receptor expression, fetal brain cDNA was used as positive control. *C*, cyclin A expression in five neuroblastoma tumors. *Lanes 1* and *3*, neuroblastomas with high cyclin A expression; *Lanes 2* and *4*, neuroblastomas with enhanced expression; *Lane 5*, neuroblastoma with no expression.

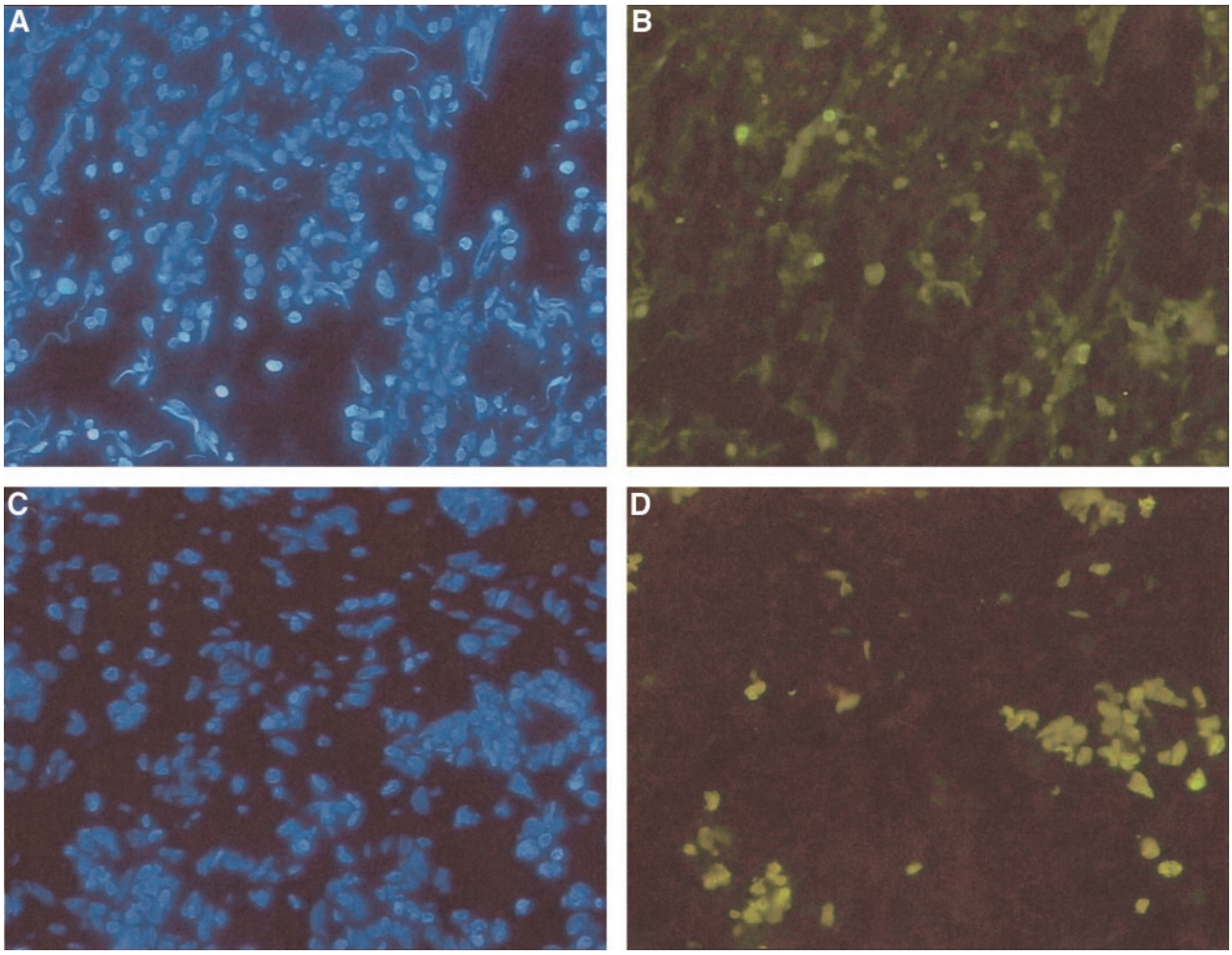

Fig. 2 Apoptosis in neuroblastomas. *A* and *B*, neuroblastoma with low AI (<0.82% TUNEL-positive cells). *C* and *D*, neuroblastoma with high AI (>0.82% TUNEL-positive cells) *A* and *C*, staining with 4′,6-diamidino-2-phenylindole-staining; *B* and *D*, TUNEL assay.

5% nonfat dry milk and 0.1% Tween 20 in Tris-buffered saline, they were incubated at room temperature for 2 h with a 1:400 dilution of a rabbit polyclonal anti-cyclin A antibody (Santa Cruz Biotechnology, Santa Cruz, CA), then with an antirabbit peroxidase-conjugated secondary antibody (Amersham). The blot was finally probed by the ECL Western blotting detection system (Amersham). Equal loading of protein was confirmed by rabbit polyclonal cdk2 antibody (Santa Cruz Biotechnology; Fig. 1).

***In Situ* End Labeling of Fragmented DNA.** The chromatin in apoptotic cells is cleaved at internucleosomal sites. To detect this fragmented DNA, we performed the TUNEL assay, using the *In Situ* Cell Death Detection kit (Boehringer Mannheim). Paraffin-embedded sections (4 μm) were deparaffinized and then incubated with proteinase K (20 μg/ml) in PBS for 15 min at 25°C. Methanol containing 0.3% H_2O_2 was applied to neutralize endogenous peroxidase. The sections were incubated with Tdt enzyme in the presence of a nucleotide mixture. After washing in PBS, the sections were stained with 4′,6-diamidino-2-phenylindole.

Apoptosis was quantitated by determining the percentage of positively stained cells within a field at a magnification of ×400. At least 1000 tumor cells were counted from 10–20 randomly chosen fields per slides assayed, and the counts were averaged to obtain the AI. For every tumor, two slides were evaluated. The median AI of all tumors examined was 0.82% (Fig. 2).

Statistical Analysis. Fisher's exact test was used to examine possible correlations between IRR expression and expression of other receptors (PCR positive *versus* negative), histology (DSR *versus* SP-D/SP-U), AI [low (≤0.82%) *versus* high (>0.82%)], proliferation [low *versus* enhanced/high (high)], *MYCN* amplification *versus* nonamplification, *MYCN* expression [low (M/A ≤0.220) *versus* high (M/A >0.220)], and clinical data (Table 2). Reported *P*s are not corrected for multiple testing.

The 6-year survival probability data for IRR, IGF-1R, TrkA, and p75NTR expression and *MYCN* amplification/expression were evaluated by the Kaplan–Meier method, and differences between survival probability curves were calculated

Table 2 Investigated neuroblastoma patients ($n = 49$) arranged according to receptor RNA expression

				MYCN		RNA[g]						
Stage[a]	Age[b]	Death[c]	Survival[d]	Amp1[e]	RNA[f]	IRR	IGF-1R	p75NTR	TrkA	Cyclin A[h]	AI[i]	Histology[j]
1	0.20	−	72.93	1	−	−	−	−	−	++	Low	3
4s	0.36	−	94.12	1	−	−	−	−	−	ND[k]	ND	3
4s	0.30	−	38.61	1	−	−	+	+	−	ND	ND	2
1	4.36	−	69.46	1	+	−	+	+	+	ND	ND	2
1	9.47	−	68.01	1	−	−	−	+	+	ND	ND	1
1	17.85	−	32.97	1	−	+	−	−	−	−	Low	1
4s	7.56	−	78.77	1	−	+	−	−	+	+	Low	3
4s	0.79	−	66.10	1	+	+	+	−	−	−	Low	3
4s	1.29	+	17.42	10	+	+	+	+	+	ND	ND	3
4s	0.69	−	113.29	1	+	+	+	+	+	ND	ND	3
4s	2.74	−	92.50	1	+	+	+	+	+	ND	ND	3
4s	2.54	−	76.73	1	+	+	+	+	+	ND	ND	2
4s	2.05	−	108.04	1	−	+	+	+	+	−	Low	3
4s	6.99	−	76.33	1	+	+	+	+	+	+	Low	3
4s	9.04	−	35.90	1	+	+	+	+	+	+	ND	3
1	4.36	−	72.30	1	+	+	+	+	+	ND	ND	3
1	11.91	−	112.99	1	−	+	+	+	+	+	High	3
1	12.94	−	66.23	1	−	+	+	+	+	−	High	3
1	18.68	−	67.91	1	+	+	+	+	+	ND	ND	3
2	0.73	−	74.58	1	+	+	+	+	+	ND	ND	3
2	5.81	−	57.82	1	−	+	+	+	+	++	High	3
2	34.06	−	130.52	32	+	+	+	+	+	−	High	3
2	116.85	+	89.60	1	−	+	+	+	+	+	High	1
3	5.97	−	14.36	1	+	+	+	+	+	+	High	3
3	9.11	−	74.45	1	−	+	+	+	+	ND	ND	3
3	10.99	−	58.77	1	+	+	+	+	+	ND	ND	3
3	16.07	−	58.94	1	+	+	+	+	+	−	High	3
3	18.74	−	141.50	1	−	+	+	+	+	+	High	3
4	19.31	−	40.66	1	−	+	+	+	+	+	High	3
4	29.44	+	23.83	1	−	+	+	+	−	+	High	3
4	10.86	+	15.38	40	+	−	+	−	−	++	Low	3
4	12.61	+	39.30	15	+	−	+	−	−	++	Low	1
4	30.56	+	8.09	1	−	−	+	−	−	−	Low	1
4	66.73	+	40.16	1	−	−	+	−	−	+	Low	1
3	11.88	−	81.15	20	+	−	+	−	−	++	High	3
3	59.17	+	92.70	1	−	−	+	+	−	+	Low	1
2	31.68	−	108.64	1	−	−	+	+	−	−	Low	1
3	95.73	−	68.01	15	+	−	+	+	+	ND	ND	2
4	66.46	+	31.71	5	+	−	+	+	+	ND	ND	3
4	57.02	+	12.57	4	+	−	−	+	+	++	High	1
2	13.63	−	90.75	1	−	−	−	+	−	−	High	1
3	30.79	−	114.11	1	−	−	−	+	−	ND	High	1
4	20.16	+	6.50	8	−	−	−	+	−	ND	ND	3
4	30.66	+	21.75	30	+	−	−	+	−	ND	ND	3
4	131.64	+	24.59	1	+	−	−	+	−	−	Low	1
2	47.45	+	18.35	1	−	−	−	−	−	+	High	2
4	34.49	+	6.60	25	+	−	−	−	−	+	Low	2
4	60.19	+	35.77	1	−	−	−	−	−	−	Low	1
4	76.20	−	111.84	1	−	−	−	−	−	−	Low	3

[a] Stage of disease at diagnosis (according to INSS criteria).
[b] Age at diagnosis in months.
[c] +, dead; −, alive.
[d] Survival time in months.
[e] Genomic amplification status of *MYCN* (1, single copy per haploid genome; >1, amplified).
[f] MYCN RNA expression (for criteria see "Materials and Methods").
[g] Receptor RNA expression status.
[h] Expression of cyclin A as parameter for the proliferation rate.
[i] High >0.82%, low ≤0.82% TUNEL-positive cells.
[j] Histology (according to Shimada criteria) with 1 = DSR; 2 = SP-D; 3 = SP-U.
[k] ND, not determined.

Table 3 Six-year survival probabilities (in months) in 49 neuroblastoma patients depending on receptor expression and other variables

Variable	6-Year survival (%)	Survival time (months) Mean	95% confidence interval	P^a
IRR				
Expression	91.8	124.6	108.0–142.3	
Nonexpression	49.7	65.3	46.9–83.7	0.003
TrkA				
Expression	88.5	121.2	102.9–139.4	
Nonexpression	46.6	64.5	45.1–83.8	0.017
p75NTR				
Expression	79.5	108.5	90.3–126.7	
Nonexpression	47.9	65.9	41.8–89.9	0.08
IGF-1R				
Expression	78.5	107.1	88.3–125.8	
Nonexpression	52.6	68.6	43.9–93.3	0.122
MYCN				
Single copy	83.5	114.6	98.4–130.8	
Amplification	27.3	49.3	19.5–79.2	<0.0001
MYCN				
Expression	65.1	92.5	71.1–113.9	
Nonexpression	75.5	104.2	83.0–125.3	0.6
Stage				
Localized (1, 2, 3)	95.7	123.1	105.1–141.1	
Metastatic (4)	12.2	35.0	17.6–52.4	<0.0001
Age at diagnosis				
<12 months	91.1	104.5	92.8–116.1	
>12 months	52.8	78.6	56.2–100.9	0.003
Histology				
DSR or SP-D	53.6	68.0	46.9–89.0	
SP-U	79.6	116.4	98.4–134.3	0.041

[a] Log-rank test.

using the log-rank test (Table 3). Multivariate analysis of IRR expression with respect to MYCN amplification, stage, age at diagnosis, *MYCN* amplification, MYCN expression, expression of other RTKs, and histology was calculated using Cox regression analyses (Table 4). $P < 0.05$ was regarded as significant. Statistical analyses was performed with the SPSS version 10.0 software (SPSS Inc.).

RESULTS

Representative experimental results are shown in Figs. 1 and 2 for the detection of *MYCN* amplification by Southern blot (Fig. 1*A*), RNA expression by reverse transcription-PCR (Fig. 1*B*), cyclin A expression by Western blot (Fig. 1*C*), and the TUNEL assay (Fig. 2) to determine the AI.

IRR Is Predominantly Expressed in Localized and Stage 4S Neuroblastomas. IRR mRNA expression was found in 25 of 49 (51%) primary human neuroblastomas. IRR was expressed in 63% of stage 1, 57% of stage 2, 56% of stage 3, and only 14% of the metastatic disease stage 4 neuroblastomas, but in 82% of disseminated stage 4S neuroblastomas.

Comparison of stages 1, 2, and 3 with stage 4 or stages 1, 2, and 4S with stages 3 and 4 IRR revealed that expression was significantly correlated with stages 1, 2, and 3 ($P = 0.016$) and stages 1, 2, and 4S ($P = 0.002$; Fig. 3).

IRR expression was seen in 70% of neuroblastomas diagnosed in infancy, but in only 35% of tumors diagnosed after the first year of life ($P = 0.022$).

IRR Is Significantly Coexpressed with IGF-1R, TrkA, and p75NTR in Human Neuroblastomas. We found a statistically significant coexpression of IRR with IGF-1R ($P < 0.001$), TrkA ($P < 0.001$), and p75NTR ($P = 0.013$; Table 2).

IGF-1R expression was found in 69% of the investigated neuroblastoma tumors, expression of TrkA in 53%, and expression of p75NTR in 71%, respectively. Similar to the IRR, TrkA was significantly correlated with an age of ≤12 month at diagnosis ($P = 0.021$). There was a trend for preferential expression of the IGF-1R in infants compared with older patients ($P = 0.071$), but p75NTR was not expressed in an age-dependent manner ($P = 0.761$).

IRR Expression Is Correlated with an Undifferentiated Histology. IRR expression was correlated with an undifferentiated histology ($P = 0.0036$), as was TrkA ($P = 0.022$). In contrast to these findings, expression of IGF-1R and p75NTR was not associated with an undifferentiated histology. As expected, deduced from the already known functions of p75NTR, expression of this receptor was correlated with a high AI ($P = 0.003$) as was coexpressed TrkA ($P = 0.003$) but not IRR or IGF-1R. Surprisingly, there was no significant correlation between expression of any of the receptors studied and the proliferation rate.

Coexpression of IRR and IGF-1R Is Correlated with an Undifferentiated Histology and a High AI. In the subgroup of IGF-1R-expressing tumors ($n = 34$), IRR coexpression was significantly associated with an undifferentiated histology ($P = 0.0017$) and a high AI ($P = 0.017$). There was no correlation of IRR/IGF-1R coexpression with the proliferation rate (Fig. 4).

IRR Expression Is Correlated with High *MYCN* Expression in *MYCN*-Nonamplified Neuroblastomas. IRR was expressed in 61% of neuroblastomas without *MYCN* amplification, but in only 18% of *MYCN*-amplified neuroblastomas ($P = 0.018$). In neuroblastomas without *MYCN* amplification, IRR expression was correlated with high *MYCN* expression ($P = 0.02$).

IRR Expression and Prognosis. IRR mRNA expression is a new prognostic marker in neuroblastoma. A 6-year survival probability of 91.8% was seen in neuroblastoma patients with IRR expression in the tumor as compared with 49.7% in patients without IRR expression in the tumor ($P = 0.003$; Table 3; Fig. 5). In a multivariate Cox regression analysis, the prognostic

Table 4 Multivariate Cox regression analysis for IRR expression with respect to different second variables

First variable	Second variable	P^a
IRR expression	Stage (1, 2, 3, *vs.* 4)	0.256
	Age at diagnosis (>12 *vs.* ≤12 month)	0.045
	Histology	0.014
	MYCN amplification	0.037
	MYCN expression	(0.005)
	IGF-1R expression	(0.014)
	TrkA expression	0.147
	p75NTR expression	(0.018)

[a] P in parentheses for variables without own prognostic impact.

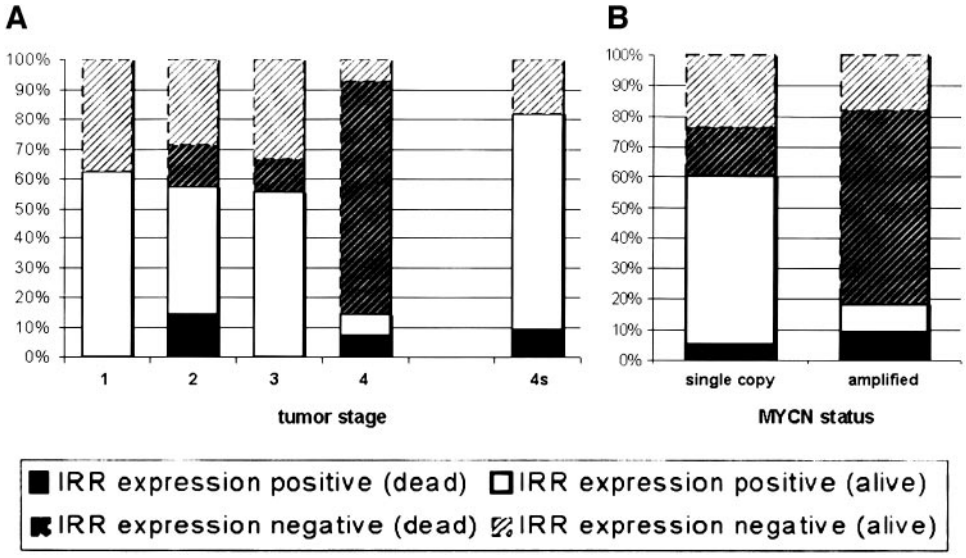

Fig. 3 IRR expression (positive) or nonexpression (negative) according to tumor stage (*A*) and MYCN status (nonamplified *versus* amplified; *B*), further differentiated by outcome (dead or still alive at the writing of the report).

impact of IRR expression was independent of *MYCN* amplification ($P = 0.037$), age at diagnosis (older than 12 months *versus* 12 months or younger; $P = 0.045$) and histological differentiation (DSR and SP-D *versus* SP-U; $P = 0.014$), but it was not independent of stage (1, 2, and 3 *versus* 4; Table 4).

Because the IRR is a heterodimerization partner for IGF-1R, we were interested in the prognostic value of IRR expression in the subgroup of IGF-1R-expressing tumors ($n = 34$). In this subgroup we found a 6-year survival probability of 90.9% for tumors that coexpressed IRR/IGF-1R-*versus* 51.9% in tumors expressing only IGF-1R ($P = 0.0108$; Fig. 5). In multivariate analysis, IRR expression was prognostically independent of IGF-1R expression ($P = 0.014$; Table 4). However, we found no correlation with apoptosis, proliferation, and differentiation for IRR expression in the subgroup of IGF-1R-nonexpressing tumors.

Prognostic Relevance of TrkA, p75NTR, and IGF-1R. TrkA expression was of prognostic significance, and p75NTR approached significance in the 49 neuroblastomas investigated in the present study ($P = 0.017$ and 0.08, respectively). IGF-1R expression was not of prognostic significance ($P = 0.122$; Table 3).

***MYCN* Gene Amplification and MYCN mRNA Expression.** The *MYCN* gene was amplified in 11 (22%) of 49 investigated neuroblastomas. MYCN mRNA expression was strongly correlated with *MYCN* amplification; thus, 10 (91%) of the 11 neuroblastomas with *MYCN* gene amplification but only 14 (37%) of 38 tumors without *MYCN* gene amplification expressed MYCN mRNA at a high level ($P = 0.002$). *MYCN* amplification significantly differentiates an unfavorable prognostic subgroup in this study ($P < 0.0001$). Expression of MYCN RNA was of no prognostic relevance in the group of 49 neuroblastomas ($P = 0.6$).

DISCUSSION

IGFs and their receptors regulate cell proliferation, differentiation, and death of normal and neoplastic cells. They have

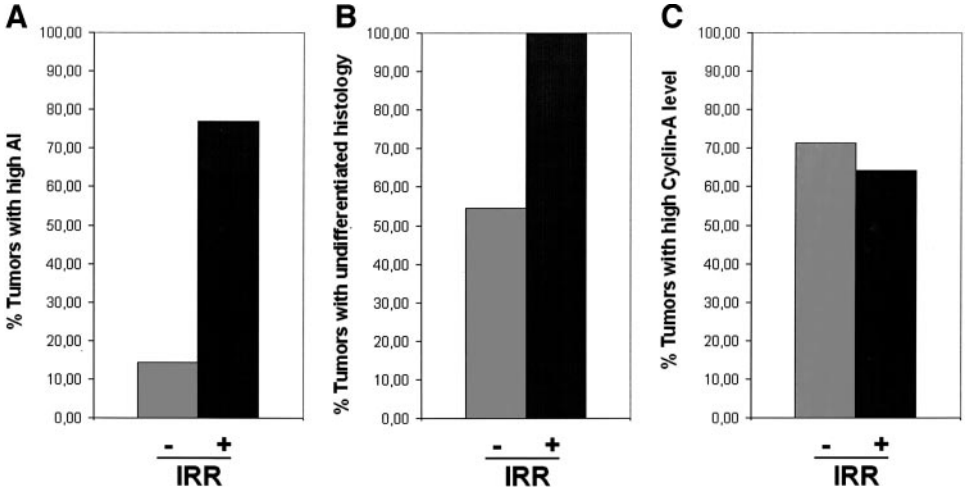

Fig. 4 Subgroups of the IGF-1R-expressing tumors ($n = 34$). IGF-1R/IRR coexpression is associated with a high AI (*A*; $P = 0.0017$) and an undifferentiated histology (*B*; $P = 0.017$). *C*, differences according to expression of the proliferation marker cyclin A are not statistically significant.

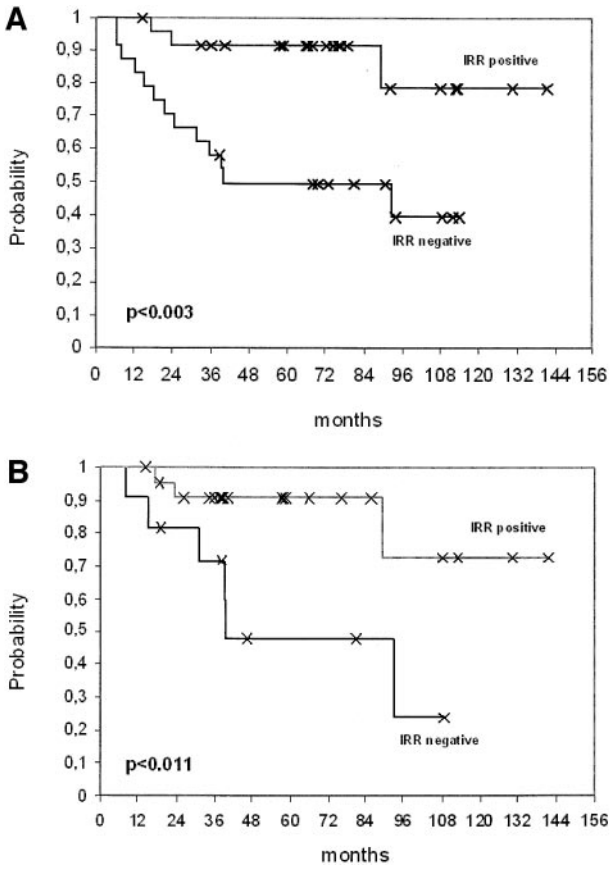

Fig. 5 *A*, Kaplan–Meier analysis for all investigated patients ($n = 49$). Survival probability of patients with IRR-expressing neuroblastomas ($n = 25$) *versus* IRR-nonexpressing neuroblastomas ($n = 24$). *B*, Kaplan–Meier analysis for patients with IGF-1R-expressing neuroblastomas ($n = 34$). Survival probability of patients with IRR coexpression ($n = 23$) *versus* IRR-noncoexpressing neuroblastomas ($n = 11$).

been implicated in the development of the nervous system and in the pathology of neuroblastoma (32, 33). Our study indicates that IRR, a new member of the IR-/IGF receptor family is differentially expressed in primary human neuroblastomas, which is suggestive for a role of the IRR in neuroblastoma biology. We also examined the expression pattern of IGF-1R, TrkA, and p75NTR, which have been previously shown to be expressed in neuroblastoma cells, to investigate the possible interaction of these receptors in concert with IRR on biological effects as proliferation, apoptosis, and differentiation.

Expression of IRR Is a New Prognostic Marker in Neuroblastoma. In the present study, IRR mRNA expression strongly correlated with a favorable outcome in neuroblastoma, which can be attributed to the close association of IRR expression with favorable tumor stages and a predominant expression in neuroblastomas diagnosed in infancy. Expression of TrkA also correlated significantly with a favorable prognosis, whereas expression of p75NTR and IGF-1R showed only a statistical trend toward a better survival probability (Table 3).

In multivariate analysis, the prognostic impact of IRR expression was statistically independent of *MYCN* amplification status and age at diagnosis, but not independent of tumor stage (Table 4).

Independency of *MYCN* amplification and age makes IRR expression interesting for further therapy stratification because at present, in stage 1, 2, 3, and 4S disease, age and *MYCN* amplification are the most commonly used parameters for stratification.

Role of IRR in Neuroblastoma Biology. Dimerization of receptor monomers at the cell surface was shown to be one early event in the activation of the RTKs, leading to autophosphorylation of intracellular domains and further activation of signaling cascades. Physiologically, dimerization is initiated by ligand binding but also by overexpression of receptor monomers exceeding a specific cell surface density threshold for autodimerization (34). We therefore examined the expression pattern of the investigated RTKs themselves and in combination with potential heterodimerization partners that might be important with respect to biological functions. Receptor expression was further compared with proliferation rate (examined by cyclin A protein expression), apoptosis (examined by the TUNEL assay), and morphological differentiation (examined by histology). We showed that IRR expression was strongly correlated with neuroblastomas with an undifferentiated histology, independent of AI and proliferation rate.

Known biological effects of IGF-1R expression in neuroblastoma cells include the induction of proliferation and downregulation of apoptosis (35–38). In contrast to these functions of IGF-1R, the expression pattern of this receptor was not associated with differentiation, proliferation rate, or apoptosis in tumor cells of primary neuroblastomas of our cohort. Missing associations between IGF-1R expression and biological functions might in part be explained by coexpression of IRR and IGF-1R. Recently, Kovacina and Roth (24) showed that these two receptors, when coexpressed, form heterodimeric receptors composed of an $\alpha\beta$-subunit of IGF-1R and another $\alpha\beta$-subunit of IRR and that these heterodimeric receptors are functional RTKs. Our correlative observations of enhanced apoptosis and undifferentiated histology in tumors expressing both receptors in contrast to tumors expressing only IGF-1R indicates an important role of IRR as a coexpression partner for IGF-1R in neuroblastoma cells. This observation is particularly important because an own ligand for IRR has to date not been found. Furthermore, the prognostic outcome of patients with IRR/IGF-1R coexpression was more favorable than that of patients expressing only IGF-1R ($P = 0.018$; Fig. 4).

In addition to IRR/IGF-1R coexpression, we found a significant coexpression of IRR and TrkA. In multivariate analysis, we showed a dependency of the prognostic impact of IRR expression on TrkA expression. This expression pattern has shown to be important for developing sympathetic and sensory neurons (20). Heterodimerization, however, has only been described for IGF-1R and not for TrkA (24).

Expression of the p75NTR was strongly correlated with a high AI but not to the proliferation rate and, in contrast to IRR, not to an undifferentiated histology; thus, it also exerts its function of inducing apoptosis in more differentiated neuroblastoma cells. Recently, it was shown that p75NTR as a member of the TNF receptor family induces apoptosis in neuroblastoma cells (39–41), which is in accordance with our results. The

significant coexpression of p75NTR with the investigated RTKs might explain the correlative trend of RTK expression linked to a higher AI. These results are in accordance with the findings of Niesler *et al.* (14), who observed potentiation of TNF-induced apoptosis by activated IGF-1R.

IRR Is Expressed in Neuroblastomas without *MYCN* Amplification and High *MYCN* Expression. In the present study, *MYCN*-amplified neuroblastomas had higher median MYCN expression compared with neuroblastomas without *MYCN* amplification, which is in accordance with the published literature (4, 5). We found that IRR mRNA expression strongly correlated with neuroblastomas without *MYCN* amplification and that within *MYCN*-nonamplified tumors, IRR was associated with high MYCN expression. This is in accordance with the findings of Cohn *et al.* (6), who described a trend toward a better prognostic outcome for neuroblastomas diagnosed in infancy without *MYCN* amplification and higher MYCN mRNA expression. Finally, these data reflect the complexity of influences on cellular functions by MYC transcription factors, because forced expression of *MYC* oncogenes induces proliferation and prevents differentiation on the one hand, but induces apoptosis on the other (42). The low frequency of IRR expression in *MYCN*-amplified tumors might reflect the developmental stage from which these *MYCN*-amplified neuroblastoma cells are derived.

We conclude that IRR might have a role in the biology and pathogenesis of human neuroblastomas. In agreement with the current literature, we hypothesize that IRR might work as a regulatory partner of IGF-1R in IGF signaling. IRR influences the physiological development of the embryonal nervous system and thus might also play a role in tumorigenesis of malignancies originating from premature neuronal cells. Furthermore, our data indicate that the assessment of IRR expression in neuroblastoma tumors at the time of diagnosis provides confirmative prognostic information, which helps in determining the most appropriate duration and intensity of treatment. Future therapeutic approaches may be aimed at influencing IRR expression in human neuroblastomas and, thus, RTK signaling pathways contributing to the activation of apoptosis.

ACKNOWLEDGMENTS

We thank our colleagues from ~100 German pediatric centers for providing us with neuroblastoma tumor material since 1980. We are grateful to Prof. Dr. Fritz Lampert, former head of the Department of Pediatric Oncology at the Justus-Liebig University of Giessen, for support of our laboratory.

REFERENCES

1. Schwab, M., Alitalo, K., Klempnauer, K. H., Varmus, H. E., Bishop, J. M., Gilbert, F., Brodeur, G., Goldstein, M., and Trent, J. Amplified DNA with limited homology to myc cellular oncogene is shared by human neuroblastoma cell lines and a neuroblastoma tumour. Nature (Lond.), *305:* 245–248, 1983.

2. Brodeur, G. M., Seeger, R. C., Schwab, M., Varmus, H. E., and Bishop, J. M. Amplification of N-myc in untreated human neuroblastomas correlates with advanced disease stage. Science (Wash. DC), *224:* 1121–1124, 1984.

3. Brodeur, G. M., Maris, J. M., Yamashiro, D. J., Hogarty, M. D., and White, P. S. Biology and genetics of human neuroblastomas. J. Pediatr. Hematol. Oncol., *19:* 93–101, 1997.

4. Seeger, R. C., Wada, R., Brodeur, G. M., Moss, T. J., Bjork, R. L., Sousa, L., and Slamon, D. J. Expression of N-myc by neuroblastomas with one or multiple copies of the oncogene. Prog. Clin. Biol. Res., *271:* 41–49, 1988.

5. Bordow, S. B., Norris, M. D., Haber, P. S., Marshall, G. M., and Haber, M. Prognostic significance of MYCN oncogene expression in childhood neuroblastoma. J. Clin. Oncol., *16:* 3286–3294, 1998.

6. Cohn, S. L., London, W. B., Huang, D., Katzenstein, H. M., Salwen, H. R., Reinhart, T., Madafiglio, J., Marshall, G. M., Norris, M. D., and Haber, M. MYCN expression is not prognostic of adverse outcome in advanced-stage neuroblastoma with nonamplified MYCN. J. Clin. Oncol., *18:* 3604–3613, 2000.

7. Nakagawara, A., Arima-Nakagawara, M., Scavarda, N. J., Azar, C. G., Cantor, A. B., and Brodeur, G. M. Association between high levels of expression of the trk gene and favorable outcome in human neuroblastoma. N. Engl. J. Med., *328:* 847–854, 1993.

8. Christiansen, H., Christiansen, N. M., Wagner, F., Altmannsberger, M., and Lampert. F. Neuroblastoma: inverse relationship between expression of N-myc and NGF-r. Oncogene, *5:* 437–440, 1990.

9. Christiansen, N. M., Christiansen, H., Berthold, F., and Lampert, F. Transcriptional activity of N-myc and ngf-r in 50 primary human neuroblastomas as predictor for clinical outcome. Int. J. Oncol., *3:* 853–857, 1993.

10. Kogner, P., Barbany, G., Dominici, C., Castello, M. A., Raschella, G., and Persson, H. Coexpression of messenger RNA for TRK protooncogene and low affinity nerve growth factor receptor in neuroblastoma with favorable prognosis. Cancer Res., *53:* 2044–2050, 1993.

11. Surmacz, E. Function of the IGF-I receptor in breast cancer. J. Mammary Gland Biol. Neoplasia, *5:* 95–105, 2000.

12. Chakravarti, A., Loeffler, J. S., and Dyson, N. J. Insulin-like growth factor receptor I mediates resistance to anti-epidermal growth factor receptor therapy in primary human glioblastoma cells through continued activation of phosphoinositide 3-kinase signaling. Cancer Res., *62:* 200–207, 2002.

13. El-Brady, O., Romanus, J. A., Helman, L. J., Cooper, M. J., Rechler, M. M., and Israel, M. A. Autonomous growth of a human neuroblastoma line mediated by insulin-like growth factor II. J. Clin. Investig., *84:* 829–839, 1989.

14. Niesler, C. U., Urso, B., Prins, J. B., and Siddle, K. IGF-I inhibits apoptosis induced by serum withdrawal, but potentiates TNF-α-induced apoptosis, in 3T3–L1 preadipocytes. J. Endocrinol., *167:* 165–174, 2000.

15. Shier, P., and Watt, V. M. Primary structure of a putative receptor for a ligand of the insulin family. J. Biol. Chem., *264:* 14605–14608, 1989.

16. Hänze, J., Berthold, A., Klammt, J., Gallaher, B., Siebler, T., Kratzsch, J., Elmlinger, M., and Kiess, W. Cloning and sequencing of the complete cDNA encoding the human insulin receptor-related receptor. Horm. Metab. Res., *31:* 77–79, 1999.

17. Zhang, B., and Roth, R. A. The insulin receptor-related receptor. Tissue expression, ligand binding specificity, and signaling capabilities. J. Biol. Chem., *267:* 18320–18328, 1992.

18. Jui, H. Y., Suzuki, Y., Accili, D., and Taylor, S. I. Expression of a cDNA encoding the human insulin receptor-related receptor. J. Biol. Chem., *269:* 22446–22452, 1994.

19. Reinhardt, R. R., Chin, E., Zhang, B., Roth, R. A., and Bondy, C. A. Insulin receptor-related receptor messenger ribonucleic acid is focally expressed in sympathetic and sensory neurons and renal distal tubule cells. Endocrinology, *133:* 3–10, 1993.

20. Reinhardt, R. R., Chin, E., Zhang, B., Roth, R. A., and Bondy, C. A. Selective coexpression of insulin receptor-related receptor (IRR) and TRK in NGF-sensitive neurons. J. Neurosci., *14:* 4674–4683, 1994.

21. Tsuji, N., Tsujimoto, K., Takada, N., Ozaki, K., Ohta, M., and Itoh, N. Expression of insulin receptor-related receptor in the rat brain examined by *in situ* hybridization and immunohistochemistry. Brain Res. Mol. Brain Res., *41:* 250–258, 1996.

22. Elmlinger, M. W., Rauschnabel, U., Koscielniak, E., Haenze, J., Ranke, M. B., Berthold, A., Klammt, J., and Kiess, W. Correlation of type I insulin-like growth factor receptor (IGF-IR) and insulin receptor-

related receptor (IRR) messenger RNA levels in tumor cell lines from pediatric tumors of neuronal origin. Regul. Pept., *84:* 37–42, 1999.

23. Moxham, C. P., and Jacobs, S. Insulin/IGF-I receptor hybrids: a mechanism for increasing receptor diversity. J. Cell. Biochem., *48:* 136–140, 1992.

24. Kovacina, K. S., and Roth, R. A. Characterization of the endogenous insulin receptor-related receptor in neuroblastomas. J. Biol. Chem., *270:* 1881–1887, 1995.

25. Soos, M. A., Whittaker, J., Lammers, R., Ullrich, A., and Siddle, K. Receptors for insulin and insulin-like growth factor-I can form hybrid dimers. Characterisation of hybrid receptors in transfected cells. Biochem. J., *270:* 383–390, 1990.

26. Seely, B. L., Reichart, D. R., Takata, Y., Yip, C., and Olefsky, J. M. A functional assessment of insulin/insulin-like growth factor-I hybrid receptors. Endocrinology, *136:* 1635–1641, 1995.

27. Brodeur, G. M., Pritchard, J., Berthold, F., Carlsen, N. L. T., Castel, V., Castleberry, R. P., De Bernardi, B., Evans, A. E., Favrot, M., Hedborg, F., Kaneko, M., Kemshead, J., Lampert, F., Lee, R. E. J., Look, A. T., Pearson, A. D. J., Philip, T., Roald, B., Sawada, T., Seeger, R. C., Tsuchida, Y., and Voute, P. A. Revisions of the international criteria for neuroblastoma diagnosis, staging, and response to treatment. J. Clin. Oncol., *11:* 1466–1477, 1993.

28. Shimada, H., Chatten, J., Newton, W. A., Sachs, N., Hamoudi, B., Chiba, T., Marsden, H. B., and Misugi, K. Histopathologic prognostic factors in neuroblastic tumors: Definition of subtypes of ganglioneuroblastoma and an age-linked classification of neuroblastomas. J. Natl. Cancer Inst. (Bethesda), *73:* 405–416, 1984.

29. Berthold, F., and Hero, B. Neuroblastoma: current drug recommendations as part of the total treatment approach. Drugs, *59:* 1261–1277, 2000.

30. Chomczynski, P., and Sacchi, N. Single-step method of RNA isolation by acid guanidinium thiocyanate-phenol-chloroform extraction. Anal. Biochem., *162:* 156–159, 1987.

31. Kinoshita, T., Imamura, J., Nagai, H., and Shimotohno, K. Quantification of gene expression over a wide range by the polymerase chain reaction. Anal. Biochem., *206:* 231–235, 1992.

32. Ishii, D. N. Neurobiology of insulin and insulin-like growth factors. *In:* S. E. Loughlin and J. H. Fallon (eds.), Neurotrophic Factors, pp. 415–442. San Diego: Academic Press, 1993.

33. Kiess, W., Koepf, G., Christiansen, H., and Blum, W. F. Human neuroblastoma cells use either insulin-like growth factor-I or insulin-like growth factor-II in an autocrine pathway via the IGF-I receptor. Regul. Pept., *72:* 19–29, 1997.

34. Hempstead, B. L., Rabin, S. J., Kaplan, L., Reid, S., Parada, L. F., and Kaplan, D. R. Overexpression of the trk tyrosine kinase rapidly accelerates nerve growth factor-induced differentiation. Neuron, *9:* 883–896, 1992.

35. Peruzzi, F., Prisco, M., Dews, M., Salomoni, P., Grassilli, E., Romano, G., Calabretta, B., and Baserga, R. Multiple signaling pathways of the insulin-like growth factor 1 receptor in protection from apoptosis. Mol. Cell. Biol., *19:* 7203–7215, 1999.

36. Kurihara, S., Hakuno, F., and Takahashi, S. Insulin-like growth factor-I-dependent signal transduction pathways leading to the induction of cell growth and differentiation of human neuroblastoma cell line SH-SY5Y: the roles of MAP kinase pathway and PI 3-kinase pathway. Endocr. J., *47:* 739–751, 2000.

37. Macaulay, V. M. Insulin-like growth factors and cancer. Br. J. Cancer, *65:* 311–320, 1992.

38. Singleton, J. R., Randolph, A. E., and Feldman, E. L. Insulin-like growth factor I receptor prevents apoptosis and enhances neuroblastoma tumorigenesis. Cancer Res., *56:* 4522–4529, 1996.

39. Bunone, G., Mariotti, A., Compagni, A., Morandi, E., and Della Valle, G. Induction of apoptosis by p75 neurotrophin receptor in human neuroblastoma cells. Oncogene, *14:* 1463–1470, 1997.

40. Kuner, P., and Hertel, C. NGF induces apoptosis in a human neuroblastoma cell line expressing the neurotrophin receptor p75NTR. J. Neurosci. Res., *54:* 465–474, 1998.

41. Bono, F., Lamarche, I., Bornia, J., Savi, P., Della Valle, G., and Herbert, J. M. Nerve growth factor (NGF) exerts its pro-apoptotic effect via the p75NTR receptor in a cell cycle-dependent manner. FEBS Lett., *457:* 93–97, 1999.

42. Bouchard, C., Staller, P., and Eilers, M. Control of cell proliferation by myc. Trends Cell Biol., *8:* 202–206, 1998.